Paper accepted for presentation at 2009 IEEE Bucharest Power Tech Conference, June 28th - July 2nd, Bucharest, Romania

Quasi-Steady-State Modeling of Interarea Oscillations

Costas D. Vournas, *Fellow IEEE* and John C. Mantzaris

***Abstract*-- The subject of this paper is the extension of QSS modeling to include low frequency interarea oscillations in power system long-term dynamics. All other electromechanical oscillations, such as local or intra-area are replaced by equilibrium (algebraic) equations. Modal analysis and simulations are made on a classical test system of 11 buses and 4 generators. The effect of solver parameters and generator models on simulation results is investigated. Modal reduction is applied to Automatic Voltage Regulators and Speed Governors resulting in four different simplified models. A comparison is made between extended QSS and detailed modeling, focusing on the accuracy of the interarea mode frequency and damping.**

***Index Terms*-- Quasi Steady State approximation, interarea oscillations, reduced order modeling, modal reduction.**

I. Introduction

INTERAREA oscillations appear between large interconnected systems and are influenced by the dynamics of speed governors and automatic voltage regulators. Damping of such oscillations is important for power system stability. In order to study these oscillations, usually systems are modeled in detail resulting in a high degree of complexity and a large amount of data to be collected.

Quasi-steady-state (QSS) simulation [1], [2] has been proven a very efficient method to analyze long-term dynamic phenomena, such as those met during on-line and off-line voltage security assessment applications. The essence of this method is to replace short-term dynamics, such as electromechanical oscillations, with their equilibrium conditions and thus transform the differential swing equations to algebraic ones that are solved together with network equations with efficiency similar to that of the power flow program. In this sense QSS simulation combines the efficiency of load flow with the advantages of time simulation.

The subject of this paper is the extension of QSS modeling to include also interarea oscillations. The proposed method is applied in a small system traditionally used for interarea oscillation studies and power system stabilizer (PSS) tuning [3], [4]. This system is presented in Fig. 1.

The paper is structured as follows: In Section II test system benchmark scenarios are formed investigating the dependence of simulation results on solution method and generator modeling accuracy. Section III is divided in two parts: in the first, single frequency QSS method [5] is summarized, while in the second part the multi-area formulation is presented and analyzed. In Section IV generator, Automatic Voltage Regulator (AVR) and Speed Governor – Steam turbine (SG-ST) dynamics are analyzed and simplified. In Section V the performance of the reduced system is evaluated, while in the last Section the conclusions are summarized.

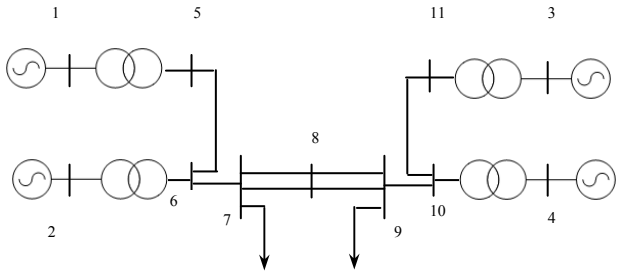

Figure 1. One line diagram of system investigated

II. Dependence of Results on Generator Modeling and Solution Methods

Before developing the extended QSS simulation method, it is necessary to define in this Section a benchmark full simulation model (including the appropriate numerical integration routine), with which to compare the reduced order model to be developed. The reason for this is that otherwise significant errors not related to the simplifications proposed in this paper may be introduced.

A. Generator modeling

Three generator models are compared in this subsection with different number of rotor windings, in order to examine the effect on electromechanical modes. For this purpose, the system of Fig. 1 is simulated with individual generator models of 6th, 4th, and 3rd order. In the first case three damper windings were included in the rotor, in the second case one damper winding, while in the third case only the field winding is represented on the generator rotor.

The state matrix eigenvalues for these models are presented in Fig.2 where the black crosses (+) mark the eigenvalues calculated using the 6th order generator models, red triangles show those of the 4th order model and blue stars (*) the eigenvalues for the 3rd order model.

As can be observed in Fig. 2, while the local electromechanical oscillation modes behave as expected, i.e. they are much better damped for the generator models with more damper windings, the interarea mode is less damped when more damper windings are modeled. This obviously contradicts the common reasoning that “more damper windings will introduce more damping” and it should be attributed to some type of modal interaction. It is noted that for other operating points of the same system, the above paradox may

C. D. Vournas is professor and J. C. Mantzaris is PhD student in the School of Electrical and Computer Engineering of National Technical University of Athens (e-mail: vournas, jmantz@power.ece.ntua.gr)

978-1-4244-2235-7/09/$25.00 ©2009 IEEE

not be present and more detailed generator models introduce in general more damping.

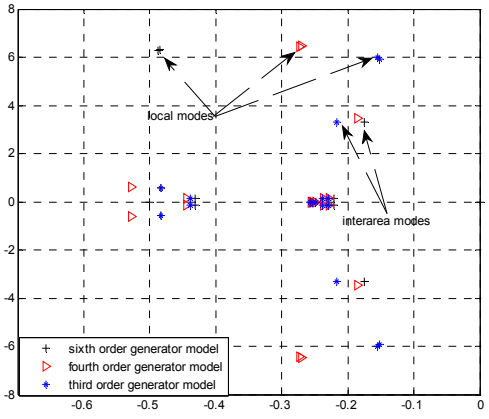

Figure 2. Comparison of eigenvalues for different generator models

In order to verify the linearization results, a 5% load increase in bus 9 was simulated with the three generator models discussed, and the active power exchanged between the two areas is shown in Fig. 3. As seen, all generator models respond with almost the same interarea oscillation frequency. Concerning oscillation damping, the more detailed the generator models, the lower the damping exhibited, as predicted by the interarea mode eigenvalues of Fig. 2. However, the differences in response are quite small, especially between the 4th and 6th order representation and they do not affect the overall response considerably.

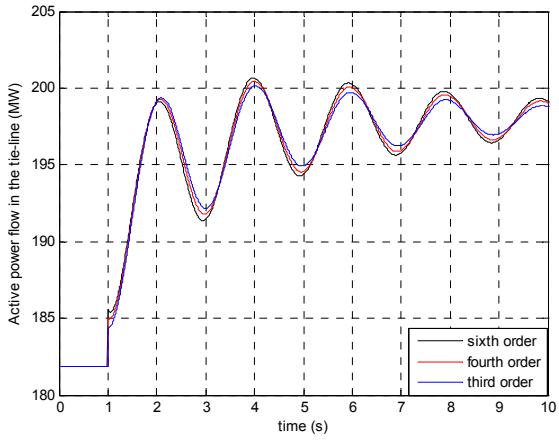

Figure 3. Interconnection active power flow for different generator models.

Since further detail in generator modeling does not contribute substantially to simulation accuracy, the 4th order generator model is taken as benchmark for further comparisons in this paper.

B. Effect of Solution methods

Another factor examined here is the accuracy of Matlab-Simulink numerical integration methods. The results obtained show a significant dependence of simulated responses on the specified numerical solution method. The same disturbance described in the previous subsection was simulated with two methods, namely ode15 (stiff/NDF) and ode23t (stiff/trapezoidal) with relative and absolute tolerance 10^{-6} and maximum step size at 0.01. The two solvers produced different results as shown in Fig. 4, which shows the active power generation of generator 4. The ode15 solution method was considered more accurate and was taken as the benchmark. The generator model used for this study was the 3rd order model with full controller representation as in Table IV of the Appendix.

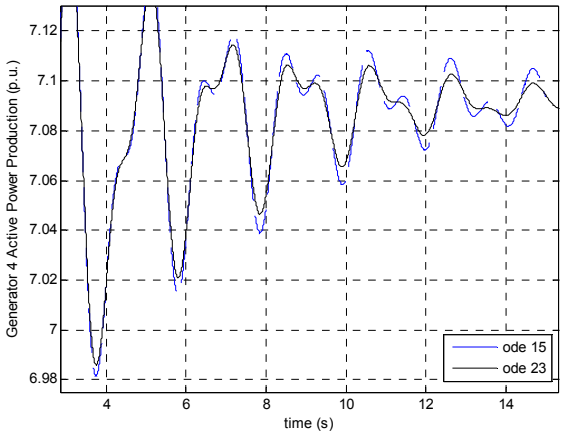

Figure 4. Comparison of dynamic response solved with different methods

III. QSS Analysis of Multi-Area System

A. Single Frequency Modeling

Before introducing the proposed modeling approach for interarea oscillations, we will review the modeling of frequency dynamics and primary governor control in QSS simulation [5]. Following Singular Perturbation Analysis [2], system dynamics are decomposed into two components. The first component, x includes slow (long-term) state variables and the second one (y) includes fast (short-term) variables, for which the differential equations are substituted by algebraic equilibrium conditions:

$$\dot{x} = f(x, y) \tag{1}$$

$$0 = g(x, y) \tag{2}$$

In this approach mechanical power output of each prime mover is considered as a (long term) state variable, while the electrical power output of generators is an algebraic variable computed together with the network equations in the same numerical solution process. The mismatch between the sum of mechanical power and the total electrical generation is the system mismatch:

$$\eta = \sum \left(P_{mi} - P_{ei} \right) \tag{3}$$

The total mismatch η is an algebraic variable that is calculated during the solution of network equations included in functions g above. The equation to match this extra variable is the angle reference, which in this paper is taken as the internal (rotor) angle of the reference machine r. Note that this is similar to the assumption of a swing bus, except that the swing bus in the traditional load flow formulation covers all of the active power mismatch (slack), while in the proposed formulation, the slack is distributed along all generators in proportion to their inertia constants:

$$\eta_i = P_{mi} - P_{ei} = \frac{H_i}{\sum H_i} \eta \tag{4}$$

The rotor angle (δ_i) of every generator (except the refer-

ence) is described through the following differential equation:

$$\varepsilon\dot{\delta}_i = \frac{1}{\omega_o}\dot{\delta}_i = \omega_i - \omega_r \tag{5}$$

where ω_o is the base electrical angular frequency and ω_r the rotor speed (per unit) of the generator selected as reference. It is clear that ω_o has a large value, so that ε is small and (5) corresponds to fast (short-term) dynamics. By taking ε to zero [2], the QSS approximation of (5) becomes:

$$\omega_i = \omega_r \tag{6}$$

In other words there is one common frequency for the system, while all rotor angles are treated as algebraic variables.

The frequency (considered common for all the system) is treated as a long-term state variable represented by the differential equation:

$$\dot{\omega}_r = \frac{\eta}{2\sum H_i} \tag{7}$$

In Fig. 5 the single frequency QSS simulation model is shown in a simplified block diagram, where SG stands for turbine and governor.

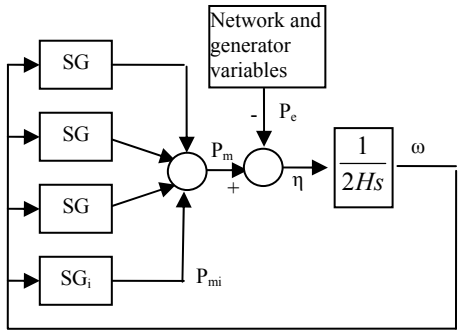

Figure 5. Simplified block diagram with common frequency assumption.

The system algebraic equations are summarized as follows:

$$g(x,y) = \begin{bmatrix} G_P \\ G_Q \\ G_G \\ G_{sys} \end{bmatrix} = \begin{bmatrix} P_m - P_{NET}(V,\theta) - \eta_i \\ Q_G(V,\theta,\delta,\mathrm{E}_f) - Q_{NET}(V,\theta) \\ P_m - P_G(V,\theta,\delta,E_f) - \eta_i \\ \delta_r \end{bmatrix} = 0 \tag{8}$$

The electrical active and reactive powers produced by each generator (P_G, Q_G) are calculated first as functions of the algebraic variables (V, θ, δ, E_f), where E_f is the excitation emf (AVR output). The same powers are then calculated also from power flow equations involving V, θ of all buses as P_{NET}, Q_{NET}.

The above system is solved by the Newton-Raphson method, using:

$$\begin{bmatrix} \theta_{j+1}^T \\ V_{j+1}^T \\ \delta_{j+1}^T \\ \eta_{j+1}^T \end{bmatrix} = \begin{bmatrix} \theta_j^T \\ V_j^T \\ \delta_j^T \\ \eta_j^T \end{bmatrix} + J_R^{-1} \begin{bmatrix} G_P^{(j)} \\ G_Q^{(j)} \\ G_G^{(j)} \\ G_{sys}^{(j)} \end{bmatrix} \tag{9}$$

where $\mathrm{J_R}$ is the Jacobian matrix $\mathrm{J_R}$:

$$\mathbf{J}_R = \begin{bmatrix} -\frac{\partial P_{NET}}{\partial\theta} & -\frac{\partial P_{NET}}{\partial V} & 0 & -\frac{\partial \eta_i}{\partial \eta} \\ \frac{\partial Q_{GN}}{\partial\theta} - \frac{\partial Q_{NET}}{\partial\theta} & \frac{\partial Q_{GN}}{\partial V} - \frac{\partial Q_{NET}}{\partial V} & \frac{\partial Q_{GN}}{\partial\delta} & 0 \\ -\frac{\partial P_G}{\partial\theta} & -\frac{\partial P_G}{\partial V} & -\frac{\partial P_G}{\partial\delta} & -\frac{\partial \eta_i}{\partial \eta} \\ 0 & 0 & e_r & 0 \end{bmatrix} \tag{10}$$

and e_r, is a row vector with 1 only on element r and all the other elements zero.

B. Extension to multiple coherent groups

The formulation proposed in this paper extends the decomposition of the previous paragraph (involving one common electrical frequency for the entire system) to represent multiple areas, each with a different frequency as long-term variable. Each predefined area A_k includes a coherent group of generators ($i \in A_k$). The decomposition to coherent groups (areas) is supposed to have been defined by one of the existing methods, e.g. [6], [7], and will not be discussed further in this paper.

Single frequency assumption holds when all electromechanical oscillations can be assumed fast (high frequency) with respect to slow variables and stable, having adequate damping. However, it is well known that large coherent groups oscillate with respect to each other giving rise to interarea oscillation of low frequency due to weak coupling with other coherent groups (areas). In this sense the dynamics of equation (5) should be re-examined for rotor angle variation between different coherent groups. In Fig. 6 a simplified block diagram of a coherent group is presented.

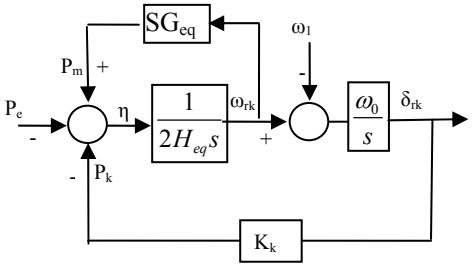

Figure 6. Simplified block diagram of a coherent group.

In Fig. 6, P_k is the active power flow from area k to the reference area, K_k is the equivalent synchronizing coefficient linking this active power flow to the angle difference between these areas considered as coherent groups. For simplicity other coherent groups are not shown in Fig. 6.

The system of Fig. 6 gives rise to an electromechanical oscillation with frequency calculated as:

$$f_{\mathrm{int}erarea} = \frac{1}{2\pi}\sqrt{\frac{K_k\omega_0}{2\mathrm{H}_{eq}}} \tag{11}$$

As seen in the above equation, in case of large coherent groups (H_{eq} large), connected with weak or stressed ties (K_k has a small value), the electromechanical oscillation frequency is low and the large value of ω_0 is compensated, as it is divided by the equivalent inertia (H_{eq}) and multiplied with K_k. This contradicts the assumption made in (5) and thus the rotor angle between coherent groups can no longer be considered as a fast (algebraic) variable.

Within each coherent group k, all intra-area and local os-

cillations are still neglected (considered fast and stable) and all rotor speeds are considered equal to one frequency ω_{rk} as in (6).

In each coherent area, one generator rotor angle δ_{rk} is taken as an area reference. This allows the solution for the area mismatch η_{area_k}. One of the area references, e.g. δ_{r1} is taken as zero (system reference angle), while all other area reference angles become long-term state variables calculated by the differential equation:

$$\dot{\delta}_{rk} = \omega_o(\omega_{rk} - \omega_{r1}) \tag{12}$$

The mechanical power produced by each generator is still a state variable as before. Figure 7 presents a simplified block diagram of a system with two coherent areas.

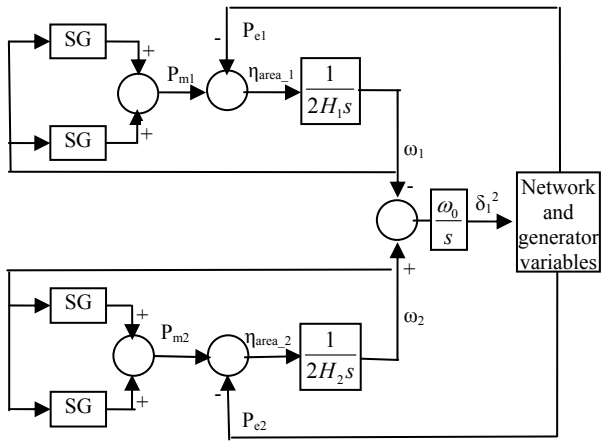

Figure 7. Simplified block diagram with multi-area formulation

Each area k has its own mismatch between mechanical and electrical power similarly to (3):

$$\eta_{area\_k} = \sum_{i \in A_k} (P_{mi} - P_{ei}) \tag{13}$$

Equations (8)-(9) are modified in the case of multi-area formulation. Variable η becomes a vector, which includes all η_{area_k} elements. Equation (10), which defines the Jacobian matrix is also modified by adding one row for each area similar to the last row of (10). The only non-zero value of vector e_k corresponds to the reference generator angle (δ_{rk}) of every coherent group.

IV. Reducing Generator And Controller Dynamics

In this Section we examine the possibilities of further model reduction after the local and intra-area modes of electromechanical oscillations have been eliminated. We proceed step by step, so in the following subsection the reduction of generator field and exciter dynamics are considered first, while we assume full modeling of speed governors and turbines. In the second subsection the reduction of the latter models is discussed.

A. Reduction of generator excitation dynamics

As discussed in Section III, in standard QSS modeling, generator dynamics are replaced with algebraic equilibrium equations. The use of (8) implies that, due to fast, high-gain AVR, the generator reaches the steady state of its field dynamics in the short-term. Under this assumption the following algebraic equation can be used to eliminate E_f in (8):

$$E_f = G\left(V_{ref} - V_t\right) \tag{14}$$

where G is the AVR steady-state gain.

The AVR model used in this paper includes, as shown in Fig. 8, a filter with a time constant T_f, the main exciter with a gain G and time constant T_e, and a differential feedback with a gain K_c and a time constant T_c. The transfer function of the AVR is thus:

$$\frac{\Delta E_f}{\Delta V} = \frac{G(1+T_c s)}{\left(1+T_f s\right)\left((1+T_e s)(1+T_c s)+GK_c s\right)} \tag{15}$$

where $\Delta V = V_{ref} - V_t$, as shown in Fig. 8.

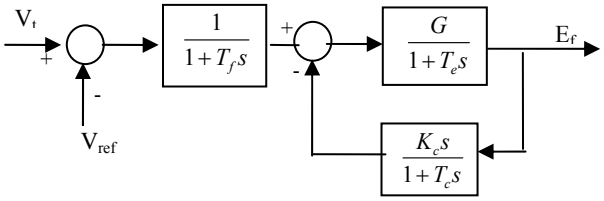

Figure 8. Automatic Voltage Regulator block diagram

The above AVR model can represent two different types of AVR, both of which are considered in the sequel: (i) a high gain AVR, for which the feedback loop of Fig.8 is open ($K_c=0$), and (ii) an AVR with transient gain reduction ($K_c \neq 0$).

1) High Gain AVR

The calculated eigenvalues of the test system with high gain AVRs are shown in Fig.9 for different degrees of generator and AVR model reduction.

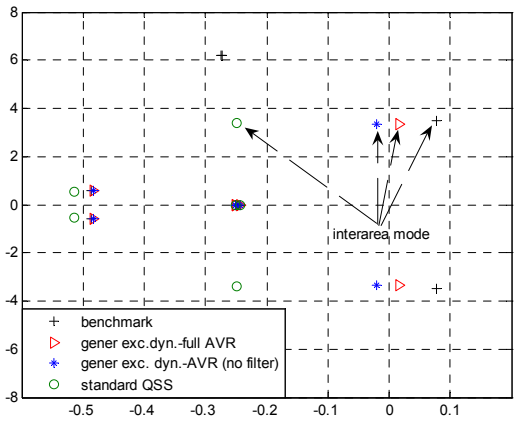

Figure 9. Eigenvalues with high gain AVR and different generator models

The standard QSS analysis (green circle), which assumes instantaneous field and excitation dynamics (algebraic representation) using (14) above, exhibits a very large error in the calculation of the interarea mode eigenvalues comparing to benchmark scenario (black cross). More specifically, the interarea oscillation mode is estimated by algebraic generator-exciter model as being well damped, while in fact for the benchmark system it is unstable.

In order to correct this major discrepancy, it is necessary to include generator excitation field and some form of AVR dynamics to the generator model to achieve a better estimate of interarea mode stability. So (8) is modified by substituting E_f with E_q', and X_d with X_d'. The emf behind transient

reactance (E_q') is now a slow state variable with dynamics given by the following differential equation:

$$T_{do}'\dot{E}_q' = -E_q' + E_f - (X_d - X_d')\cdot i_d(V,\theta,E_q') \qquad (17)$$

Regarding the high-gain AVR two alternative models are considered: full AVR modeling (red triangle), and a reduced model (blue star), which neglects the filter time constant.

As seen in Fig. 9, with the generator field dynamics explicitly represented the interarea mode damping is much better estimated. However, even with the full AVR model, there is some error introduced in damping, which is due to the elimination of the local oscillation modes. In other words, in the considered case, the local modes tend to reduce the damping of the interarea mode.

Considering the reduction of the filter time constant, even though its value is very small (0.05 s) it is seen to introduce a small, but substantial error in damping estimation. This is a problem to consider when deciding on the desired degree of model reduction, as we will see also for other controller components.

2) AVR with Transient Gain Reduction (TGR)

In this paragraph we examine the system with the four generator AVRs having transient gain reduction achieved through the differential feedback with the values of Table IV of the Appendix.

As before, two levels of AVR simplification are examined. The first simplification is to neglect the exciter time constant T_e. Although this time constant is larger than the filter time constant (T_f), its contribution to the closed loop transfer function is overrun by the differential feedback giving rise to a pole far from the frequency range of interest, as seen in Table I.

The second simplification, neglects also the time constant of the filter, same as in the high-gain AVR.

In Figs. 10 and 11 the bode diagrams of the AVR transfer function are presented. As seen, in the frequency range of interarea oscillations (~3 r/s) there is no significant variation on the gain for both simplified models. On the other hand, the simplifications introduce an error in the transfer function phase, especially when neglecting the filter time constant.

TABLE I :AVR POLES AND ZEROS

	Full AVR	Simplification 1	Simplification 2
Poles	-0.0415	-0.0417	-0.0417
	-20	-20	
	-60.2085		
Zeros	-2.5	-2.5	-2.5

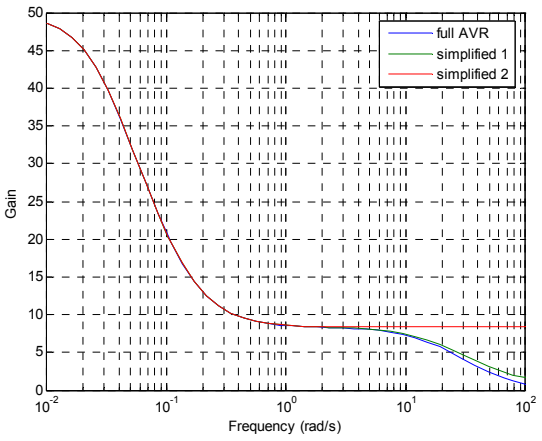

Figure 10. Bode diagram for gain of full and simplified AVR models

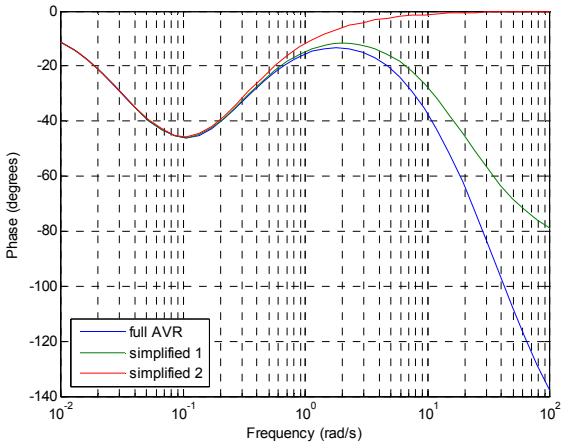

Figure 11. Bode diagram for phase of full and simplified AVR models

B. Speed Governor – Steam Turbine Modeling (SG-ST)

The block diagram of speed governor and steam turbine is shown in Fig. 12. The steam turbine consists of three stages. A part of mechanical power (F_{hp}) is produced by the high pressure turbine with a time constant (T_{hp}); steam is reheated (time constant T_r), and a second part of mechanical power (F_{mp}) is produced by the medium pressure steam turbine; the remaining part of mechanical power is produced by the low pressure steam turbine with time constant (T_{bp}). The corresponding transfer function is:

$$\frac{\Delta P_m}{\Delta\omega} = \frac{F_{hp}T_rT_{bp}s^2 + (F_{hp}(T_r+T_{bp}) + F_{mp}T_{bp})s + 1}{(1+T_{sm}s)(1+T_{hp}s)(1+T_rs)(1+T_{bp}s)} \qquad (17)$$

This transfer function includes also the speed governor time constant (T_{sm}).

Again two simplifications are proposed: The first neglects the low pressure time constant (T_{bp}), which eliminates a pole and a zero in the transfer function, which are effectively canceling each other. The second simplification neglects also the speed governor time constant. Poles and zeros of SG-ST of full and simplified representation are shown in Table II.

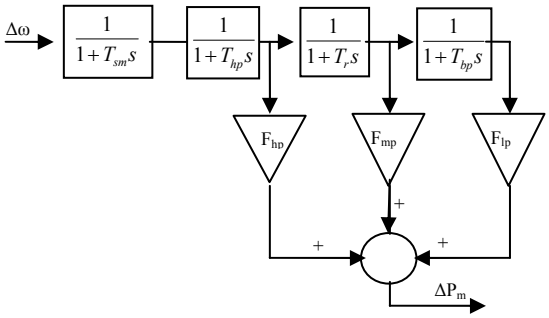

Figure 12. Speed governor – steam turbine block diagram

TABLE II
SG-ST POLES AND ZEROS

	Full SG-ST	Simplification 1	Simplification 2
Poles	-0.25	-0.25	-0.25
	-3.33	-5	-5
	-5	-10	
	-10		
Zeros	-0.6724	-0.6724	-0.6724
	-3.0985		

In Figs. 13 and 14 the bode diagrams of governor-turbine transfer functions are presented. As seen, in the frequency range of interarea oscillations (~3 r/s) there is no significant variation on the calculated gain. On the other hand, the second simplification introduces a major error in the transfer function phase.

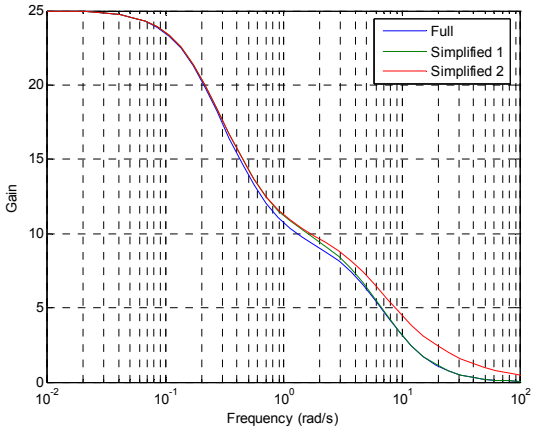

Figure 13. Bode diagram for gain of full and simplified SG-ST models

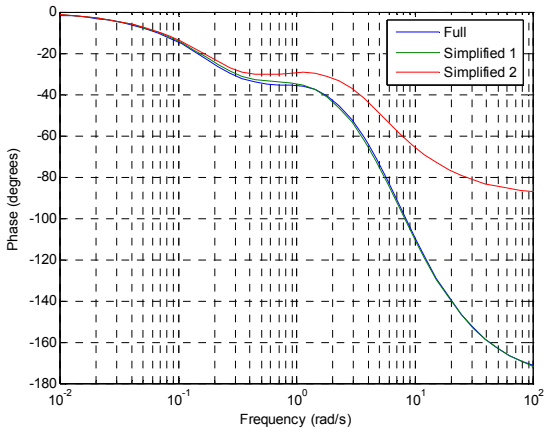

Figure14. Bode diagram for phase of full and simplified SG-ST models

In order to examine the effect of this phase error in the interarea mode damping, the phasor of mechanical torque at the interarea oscillation frequency is calculated and shown in Fig.15. As seen in this figure, the first simplification does not modify the damping torque introduced at the interarea oscillation frequency. However, the second simplification introduces extra damping to this mode as the projection on the Δω axis shows.

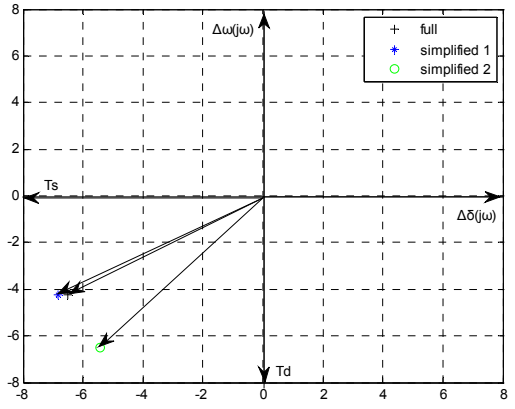

Figure 15. Interarea mode damping and synchronizing torques due to governor-turbine.

V. Performance Evaluation of the Reduced System

We have already seen that the assumption of coherent groups introduces a small error, since the local modes contribute to interarea mode damping. In this section we evaluate the overall performance of a reduced order system for which we simplify also the controller representation, as described above. The test system eigenvalues assuming AVRs with Transient Gain Reduction in all generators and the governor turbine model described above are shown in Fig. 16.

The results of the eigenvalue analysis are confirmed by the simulation of disturbance of section II, which is presented in Fig. 17.

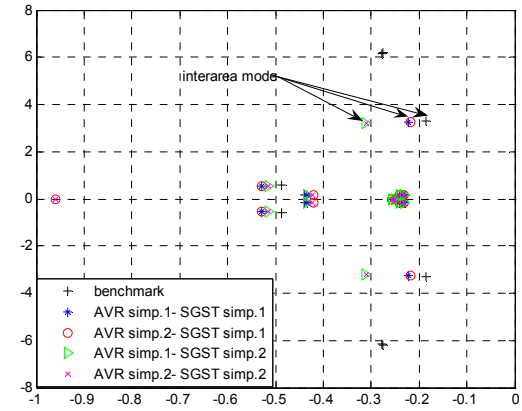

Fig. 16. Eigenvalue comparison with AVR and SG-ST simplified models.

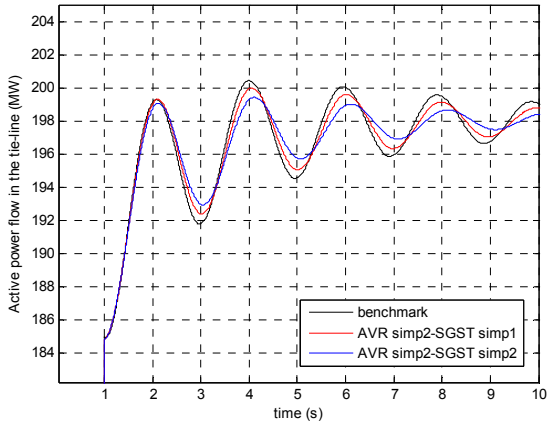

Figure 17. Active power flow in the tie-line for different representations.

The benchmark in all cases is the system with 4th order generator models with full representation of AVR and governor/turbines. As can be observed in Table III and Fig. 17, simplification 2 of the AVR (omission of filter time constant) moves slightly the interarea mode to the right (reduced damping), but this difference is very small. On the other hand, the omission of the governor time constant is moving the interarea eigenvalues to the left (additional damping). Thus, damping is overestimated if the governor time constant is neglected. The effect of model reduction to other eigenvalues is relatively small.

The frequency of the interarea oscillations is accurately estimated in all cases, but there is a small error introduced in the estimated damping. However, the overall performance of the reduced model is acceptable for system studies.

One difficulty encountered is that relatively small time constants, such as the voltage measurement filter of the AVR, or the governor time constant, have a significant impact on interarea oscillation damping and thus they cannot be simplified in all cases. This increases the complexity of the overall model, which however is still much simpler, as all local and intra-area modes have been eliminated.

TABLE III
EIGENVALUES FOR DIFFERENT DEGREES OF CONTROLLER SIMPLIFICATION

	Interarea mode	Frequency (Hz)	Damping (%)
Benchmark	-0.185 ± 3.308i	0.5265	5.6
AVR simp1-SGST simp1	-0.221 ± 3.252i	0.5176	6.8
AVR simp2-SGST simp1	-0.219 ± 3.263i	0.5193	6.7
AVR simp1-SGST simp2	-0.312 ± 3.190i	0.5077	9.8
AVR simp2-SGST simp2	-0.310 ± 3.201i	0.5094	9.6

VI. CONCLUSIONS

In this paper QSS modeling was extended to include also slow interarea oscillations. Before this, the performance of certain Matlab solvers was investigated and it was seen that they can introduce significant error in simulation results. It was also seen that for the operating point examined, the damping of the interarea mode decreases when more damper windings are introduced in the generators model.

Control devices (AVR and governor-turbines) contribute significantly in the interarea mode. Models of control devices and turbines can be simplified but certain small time constants (in the order 0.05 to 0.10 seconds) have to be maintained to achieve good accuracy in interarea mode damping. It was seen that this is due to the transfer function phase that affects the damping torque components.

It was seen also that the local electromechanical modes neglected in the QSS modeling can contribute to the damping of the interarea mode. Thus our simplified modeling of interarea modes may provide an overestimation of systems damping, which, however, remains within acceptable limits.

In general, the proposed method, avoids the complexity of full system modeling by using the QSS method, while on the other hand it represents low frequency electromechanical (interarea) oscillations with acceptable accuracy of frequency and damping. The model can be used to increase the accuracy of QSS single frequency simulation in autonomous systems with interarea modes, as well as for the design of stabilizers for interarea modes in large interconnections, without the need to include all local and intra-area modes.

APPENDIX

In the Appendix parameters are shown in per unit system unless otherwise specified.

TABLE IV
TEST SYSTEM PARAMETERS

Generator parameters		S_{nom} (MW)	H	X_d	X_d'	X_q	X_q'
		900	6.5	1.8	0.305	1.7	0.787
		T_d	T_q				
		9.3224	0.3256				
AVR		G	T_e (s)	T_c (s)	T_f (s)	K_e	
a.	TGR	50	0.1	4	0.05	0.4	
b.	High Gain			-		0	
Speed Governor		S_{nom} (MW)	R	T_{sm} (s)			
		900	0.04	0.1			
Steam Turbines		P_{nom} (MW)	T_{hp}(s)	F_{hp}	T_r(s)	F_{mp}	T_{bp}(s)
		850	0.2	0.4	4	0.3	0.3
		F_{lp}					
		0.3					

TABLE V
TEST SYSTEM OPERATING POINT

Bus number	P (MW)	Q (MW)	V (p.u.)	θ (degrees)
1	700.0	178.9	1.03	26.8
2	700.0	220.0	1.01	17.1
3	700.0	168.8	1.03	0.0
4	718.5	185.0	1.01	-10.2
5	0.0	0.0	1.007	20.4
6	0.0	0.0	0.981	10.3
7	-967	-100	0.965	2.0
8	0.0	0.0	0.954	-11.8
9	-1767	-100	0.976	-25.2
10	0.0	0.0	0.986	-16.9
11	0.0	0.0	1.01	-6.6

REFERENCES

[1] T. Van Cutsem, C. D. Vournas, "Voltage Stability of Electric Power Systems", Kluwer Academic Publishers, 1998.

[2] P.V. Kokotovic, J. O. Reilly, H. K. Khalil, Singular Perturbation Methods in Control: Analysis and Design, Inc. Orlando, 1986

[3] P. Kundur, "Power System Stability and Control", EPRI Power System Engineering Series, EPRI/McGraw-Hill, 1994.

[4] G. Rogers, "Power System Oscillations", Kluwer, Norwell, 2000.

[5] M.-E. Grenier, D. Lefebvre, T. Van Cutsem. "Quasi steady-state models for long-term voltage and frequency dynamics simulation", IEEE Power Tech Proceedings, St. Petersburg, Russia, June 2005.

[6] J. H. Chow, et al., "Inertial and Slow Coherency Aggregation for Power System Dynamic Model Reduction, IEEE Trans. on Power Systems, vol. 10, May 1995, pp. 680-685.

[7] H. You, V. Vittal, X. Wang, "Slow Coherency-Based Islanding", IEEE Trans. on Power Systems, vol. 19, Feb. 2004, pp. 483-491.